# Simultaneous line Raman/Rayleigh measurements for mixture fraction determination in turbulent, partially premixed slot burner flames

**S. Kruse[1]*, E. Varea[1], A. M. Elbaz[2], M. S. Mansour[3], G. Grünefeld[4], H. Pitsch[1]**

[1]Institute for Combustion Technology, RWTH Aachen University, Templergraben 64, 52062 Aachen, Germany
[2]King Abdullah University of Science and Technology (KAUST), Saudi Arabia
[3]Mechanical Engineering Department, The American University in Cairo, Egypt
[4]Institute of Technical Thermodynamics, RWTH Aachen University, Schinkelstraße 8, 52062 Aachen, Germany

## Abstract
In many applied combustion systems, fuel and air are neither homogeneously mixed nor fully separated before reactions occur. Mixture fraction statistics expressed as mean and fluctuation root mean square seem appropriate quantities for partially premixed flame characterization in a regime diagram [1]. In order to measure the mixture fraction and the temperature in turbulent partially premixed slot burner flames, a simultaneous, one dimensional Raman and Rayleigh technique is applied in this study. Averaged mixture fractions and their fluctuations determined in the unburnt region at different flame positions are plotted in the regime diagram. It is found that the Reynolds number has only insignificant effects on partially premixed flame stability, while time for mixing is the driving parameter to stabilize partially premixed flames.

## Introduction
For combustion processes, mixing of fuel and air is an essential parameter. Based on the mixing, combustion is classified in three different modes. In premixed combustion, fuel and air are homogeneously mixed and mixture fraction gradients are inexistent.

The flame propagates to the unburnt fuel air mixture and is located at the position where the velocity of the unburnt gas stream equals the burning velocity of the flame. The important parameters are the flame speed and the flame thickness. Non-premixed combustion is characterized by a separation of fuel and air. The diffusion of fuel and air into each other is the determining mechanism. The flame zone is stabilized at the position of stoichiometric mixture fraction. This mode is characterized by chemical and flow time scales and specifically by the rate of molecular mixing expressed by the mixture fraction dissipation rate [2].

This classification of premixed and diffusion combustion is becoming less relevant for prevalent combustion systems [3]. In most modern combustion devices, fuel and air are introduced partially premixed to the combustor to achieve better flame stabilization behavior, lower emissions and lower fuel consumption by overall lean combustion [4,5]. According to Masri [6], "partially premixed" refers to the inhomogeneity of fuel and air mixture covering a wide range of mixture fractions within and outside the flammability limits. Thus, the definition of partially premixed flames implies the existence of mixture fraction gradients [6]. Due to these mixture fractions variations in partially premixed flames, this combustion mode cannot be represented in a single regime [1].

According to the regime diagrams for premixed and non-premixed combustion, which classify these combustion modes by velocity as well as length scales [7,8] and time scales [9], mean mixture fraction and the mixture fraction fluctuations are used for classification of partially premixed flames [1]. Eight different regimes are introduced [1] related to flame structure and flame stability. The diagram enables a quantitative description of influencing factor on partially premixed flames.

Here, the effects of mixing time scales, Reynolds number and degree of premixing on turbulent partially premixed flames are investigated and their effect on partially premixed flame stability are evaluated. Measurements of turbulent partially premixed flames have been performed in wide variety of experimental setups [3, 10-13]. However, to the authors' knowledge, the effects of these on flame stability of partially premixed flames have not been described quantitatively yet.

Stratified flames which are counted as a special case of partially premixed flames [6] have been studied in different burners with two concentric fuel air streams of different equivalence ratios [10,11]. Meares and Masri [3] proposed a modification of the well-known Sydney piloted burner [12,13] for partially premixed flame investigations. The burner consists of two concentric arranged tubes, where the inner tube is for fuel supply and can be moved back forth within the surrounding air tube. This allows to change the degree of premixing at the nozzle exit. The outer tube is shrouded by a pilot stream [3]. This is similar to the earlier developed partially premixed burner by Mansour [14]. A slot burner for turbulent stratified flame investigations is applied by Barlow et al. [15]. A simultaneous line imaged Raman-, Rayleigh and CO-LIF technique is applied to detect the major species and equivalence ratio gradients in low-stretch stratified flames.

In this study, a modified slot burner is used for turbulent partially premixed flame investigations. The

* Corresponding author: s.kruse@itv.rwth-aachen.de

turbulent flame is located above the main slit. In order to generate a partially premixed fuel air stream, the fresh gases are separated by an insert in the main slit to a defined distance upstream the burner exit. The flame is stabilized by laminar pilot flames located on both side of the main slot.

Simultaneous radial profile measurements of temperature and species concentrations are conducted using a line Raman/Rayleigh technique [16]. In order to evaluate the effects of the Reynolds number and the degree of premixing on partially premixed flame stability, the mixture fraction fluctuations and the mean mixture fraction values are determined and plotted in the regime diagram.

**Experimental setup**

A modified piloted slot burner, shown in Figure 1, is used to generate turbulent partially premixed flames. The modified design of the burner allows the variation of the degree of fuel and air premixing at the burner exit. The measurements are conducted at different jet Reynolds numbers, equivalence ratios, and axial positions downstream the burner exit.

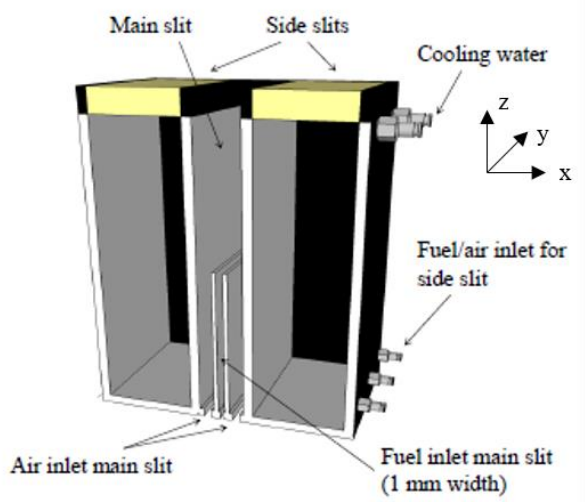


**Figure 1: Sectional view of slot burner**

The burner consists of a main slot surrounded by laminar pilot flames at both sides. The size of the pilot flames at both sides is 24 mm x 105 mm. The pilot flames are generated at the top of water cooled perforated ceramic plates. The main slot size is 12 mm x 105 mm. The hot exhaust gases of the laminar pilot flames stabilize and keep the main turbulent flames attached to the main slot.

The partially premixed fuel air flow is generated within the main slot. At the bottom plate of the main slot, three slits are used for separated fuel and air supply. An insert of two connected steel sheets separates three streams of fuel at the center and air through the two surrounding slits, as shown in Figure 1.

While fuel is supplied through the central 1 mm wide slit, the air flow passes through 4.5 mm wide slits located on both sides of the fuel slit. In order to vary the degree of premixing of the air and fuel flow at the burner exit, inserts of different lengths can be placed in the main slot. For the non-premixed case, the height of the insert is the same as the height of the main slot. On the other hand for the premixed case no insert is used. Partially premixed cases can thus be achieved by using inserts with heights smaller than the main slot height. The insert height controls the degree of partial mixing. In this study, an insert with a height of 48 mm which corresponds to 50% of the main slot height is used.

In order to investigate the mixture and temperature fields in the turbulent flame, a simultaneous, one dimensional Rayleigh Raman technique is applied [16]. The experimental setup is shown in Figure 2.

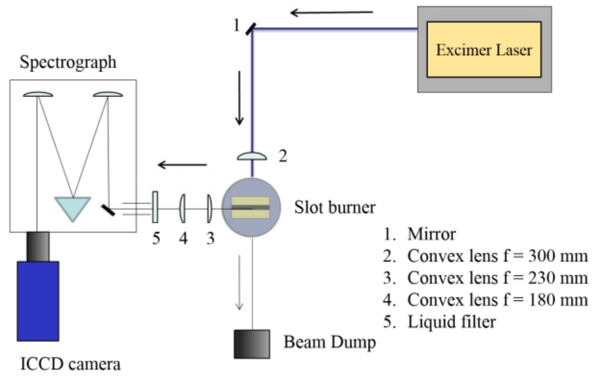


**Figure 2 Experimental setup for simultaneous Raman/Rayleigh measurements**

A KrF-Excimer Laser (EMG 150, LambdaPhysics) generates a pulsed 248 nm laser beam with an energy of 225 mJ and a repetition rate of 2 Hz. The beam is focused by a 300 mm (2) focal length lens 4 mm off-center of the main slit. Thereby, the field of view covers the range from the burner center up to 8 mm in the x-direction (Figure 1). For the scattered light collection, a lens (3) with a focal length of 230 mm is used. The collected light is focused on the slit of a spectrograph (1800 grids/mm, blaze wavelength: 250 nm, Chromex 250) by a third 180 mm focal length lens (4). The Raman spectra are imaged by a CCD camera (Dynamight, LaVision). In order to detect the Raman and Rayleigh signal intensity at the same order of magnitude, a buthylacetate filter (5) is placed in front of the spectrograph that decreases the Rayleigh signal by roughly a factor of 1/1000. The optical arrangement results in a spatial resolution of 0.75 mm and a field of view of 8 mm along the laser beam axis. In order to avoid any optical adjustments to measure at different positions above the burner exit, the burner is mounted on an xyz-table.

To generate a broad set of experimental data, three different equivalence ratio three different Reynolds numbers were investigated at three different positions above the burner. All parameters were varied independently resulting in 27 different measurement points. The experimental boundary conditions are listed in Table 1.

**Table 1 Experimental boundary conditions**

| | | | |
|---|---|---|---|
| Equivalence ratio [-] | 0.8 | 1.0 | 1.1 |
| Reynolds number [-] | 3500 | 5250 | 7500 |
| Measurement position above burner exit [mm] | 1.5 | 3.0 | 4.5 |

For signal calibration and setup validation, a heated nozzle and a McKenna-burner are used.

For the pure gas calibration of $CO_2$, $N_2$, $O_2$ and three different mixtures of $CH_4$ and $N_2$, a heating system is used to increase the gas temperature stepwise to a maximum temperature of 673 K. Raman and Rayleigh signals are detected 2 mm downstream the nozzle for various exit temperatures. This procedure allows to evaluate a temperature dependent calibration factor for the Raman cross section changes due to temperature increase. Moreover, a correlation factor between camera signal and Rayleigh cross section for each of the pure cases is defined. Figure 3 shows the signal increase of the $CO_2$ with temperature.

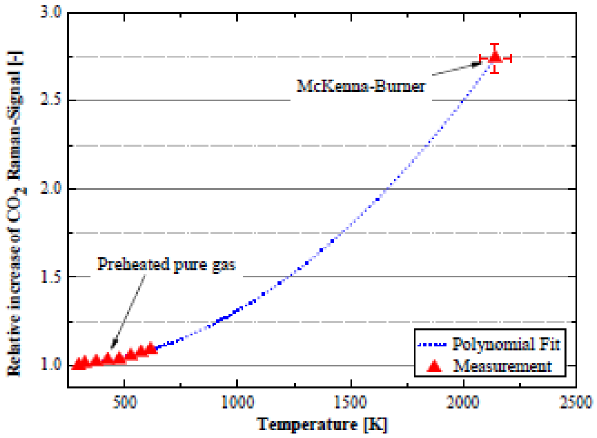


**Figure 3 Temperature dependence of $CO_2$ Raman cross section**

In order to evaluate the Raman cross section temperature dependence at higher temperature and determine a signal correlation factor for $H_2O$, Raman and Rayleigh measurements were performed at various position above the McKenna-burner.

A polynomial fit function is determined to calculate the temperature-dependent change of the Raman cross section in a wide temperature range.

Besides the determination of signal correlation, measurement points were used for the post processing validation. Therefore, simultaneous Rayleigh and Raman measurements were conducted at a position 15 mm downstream the burner plate. The temperature and species concentration at this position were calculated with 1D simulations. Figure 4 compares the measured temperatures along the beam axis and the calculated values. Note, that this point has not been used for calibration. Good agreement between experiment and simulation is found.

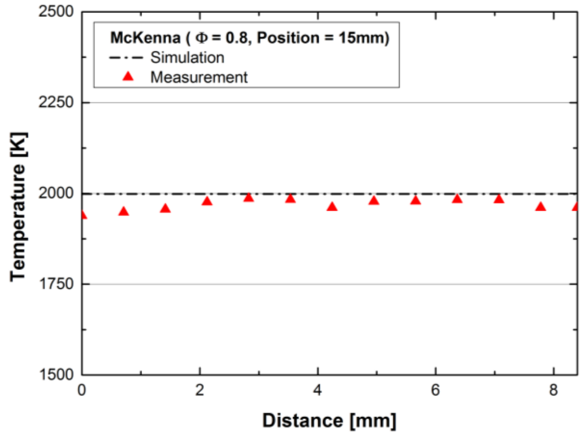


**Figure 4 Comparison measured and calculated temperature in McKenna-flame ($\phi$ = 0.8)**

**Regime diagram**

Partially premixed combustion is characterized by fluctuations of mixture fraction ranging from non-premixed to homogeneously premixed conditions inside and outside the flammability limits. Therefore, partially premixed flames cannot be described by one regime or one combustion model. A new regime diagram was recently developed by Mansour [1]. In this section, the diagram is briefly discussed. A detailed discussion of the different regimes can be found in [1]. Since mixing is essential for the definition of combustion modes, the fluctuation of mixture fraction and the averaged mixture fraction are used to classify the regimes of the partially premixed flames. A dimensionless mean mixture fraction is described by the average of the maximum and the minimum mixture fraction ($Z_{max}$ and $Z_{min}$) divided by the lean and rich mixture fraction at the flammability limit, $Z_R$ and $Z_L$, yielding

$$R_Z = \frac{Z_{max}+Z_{min}}{Z_R+Z_L} \qquad \text{Eq. 1.}$$

The dimensionless mixture fraction fluctuation $R_\Delta$ is defined as

$$R_\Delta = \frac{Z_{max}-Z_{min}}{Z_R-Z_L} \qquad \text{Eq. 2.}$$

In the regime diagram, the mean mixture fraction $R_Z$ is plotted on the y-axis, the mixture fraction fluctuation $R_\Delta$ is plotted on the x-axis. In the fully premixed mode, the mixture fraction fluctuations $R_\Delta$ are zero, while $Z_{max}$ = $Z_{min}$ are constant given by the equivalence ratio. Therefore, the premixed regime is represented by the y-axis. For non-premixed combustion, $Z_{min}$ and $Z_{max}$ are equal to 0 and 1, for pure air and pure fuel conditions, respectively. Thus, the non-premixed regime is identified by one point in the diagram. Besides the premixed and non-premixed regimes, eight partially premixed regimes exist (Figure 5). The partially premixed flames are characterized by inhomogeneities of

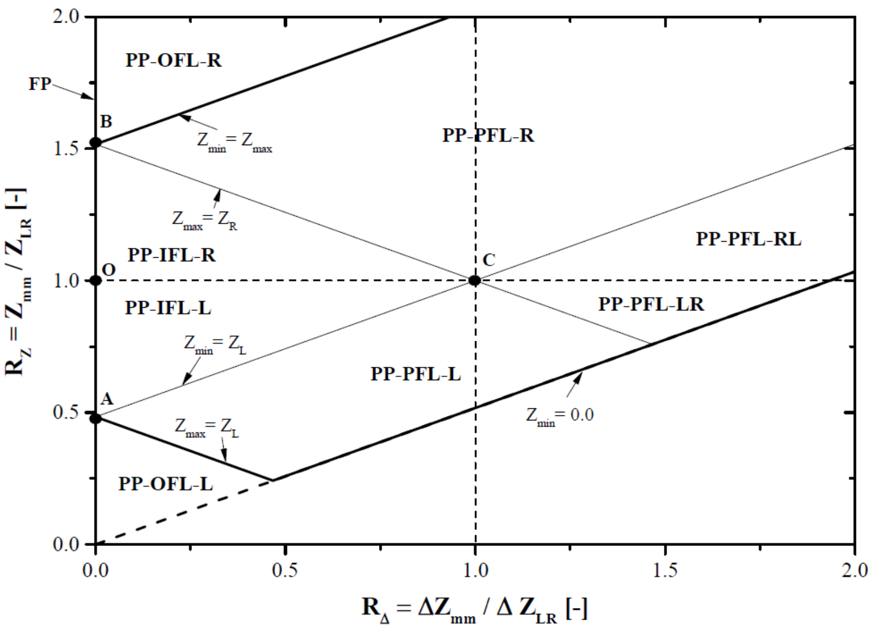


**Figure 5 Regime Diagram for partially premixed flames**

mixture fraction, where pockets of various stoichiometries can exceed the flammability limits.

However, combustion cannot occur for $Z_{min} < 0$ and $Z_{min} > Z_R$. These two conditions define the upper and lower limits of the regime diagram, all other regimes discussed below are located in-between.

In the most stable regime, the mixture fraction field is within the flammability limits, thus $Z_{min} \geq Z_L$ and $Z_{max} \leq Z_R$. The regime is indicated by the triangle A-B-C and is named partially premixed regime inside the flammability limit (PP-IFL). The values of $R_\Delta$ and $R_Z$ for the points A, B, C are summarized in Table 2.

**Table 2 $R_Z$ and $R_\Delta$ for points A, B and C**

| A | B | C |
|---|---|---|
| $Z_{min} = Z_{max} = Z_L$ | $Z_{min} = Z_{max} = Z_R$ | $Z_{min} = Z_L$ and $Z_{max} = Z_R$ |
| $R_{Z,A} = \frac{2 \times Z_{min}}{Z_R + Z_L}$ | $R_{Z,B} = \frac{2 \times Z_{max}}{Z_R + Z_L}$ | $R_{Z,C} = 1$ |
| $R_{\Delta,A} = 0$ | $R_{\Delta,B} = 0$ | $R_{\Delta,C} = 1$ |

This regime can be divided in two sub-regimes. The point O is defined as the mean of $R_{Z,A}$ and $R_{Z,B}$ (Eq. 3)

$$R_{Z,O} = \frac{R_{Z,A} + R_{Z,B}}{2} = 1$$
$$R_{\Delta,O} = 0 \qquad \text{Eq. 3.}$$

The line between O and C divides the PP-IFL into an area above the line, where the mean mixture fraction is richer, and a region below the line with leaner pockets. These regimes are called partially premixed regime inside the flammability limit rich and lean, PP-IFL-R and PP-IFL-L, respectively.

In case of $Z_{max} < Z_L$ or $Z_{min} > Z_R$, the complete mixture fraction field is outside the flammability limits. The two regimes are named PP-OFL-L and PP-OFL-R in the diagram (Partially Premixed Outside the Flammability Limit - lean and rich, respectively). For the PP-OFL-R regime, combustion can occur if environmental air dilutes the partially premixed fuel/air flow, and thereby forms mixture fraction pockets leaner than the rich flammability limit.

Furthermore, four sub-regimes are introduced, where the mixture fraction field is partially inside and partially outside the flammability limits (PP-PFL). The conditions for these regimes are described by

$$Z_{min} \leq Z_R \qquad \text{Eq. 4a}$$
$$Z_{min} \leq 0 \qquad \text{Eq. 4b}$$
$$Z_{max} \geq Z_L \qquad \text{Eq. 4c.}$$

For the first sub-regime (PP-PFL-R), the mixture field is within the flammability limits or exceeds the rich limit. The corresponding regime, in which the mixture is inside the flammability limits or falls below the lean flammability limit is named PP-PFL-L.

For the two other sub-regimes, the mixture fraction field is inside the flammability limits or exceeds both limits. These regimes are characterized by their mean mixture fraction. Consequently, for $R_Z < 1$ the regime is named PP-PFL-LR and for $R_Z > 1$ the regime is named PP-PFL-RL.

**Results and discussion**

In this section, the analyzing procedure is described and the influences of equivalence ratio, time for mixing and Reynolds number on partially premixed flames is evaluated. Each set of measurements contains 500 single images of the Raman/Rayleigh spectra. The mixture fractions and temperature profiles for each single image are determined by a post-processing routine. Temperature and molecule concentrations are calculated iteratively until the post-processing loop converges. This procedure allows to account for temperature dependent changes of the Raman cross section. The molecule concentration provides the mixture fraction. Afterwards, a filter is applied to the experimental data in order to consider only mixture fractions at temperatures below 500 K for the further analysis. The temperature limit is chosen such that only mixture fractions for unburnt conditions are analyzed. Cumulative distribution functions (CDF) are generated for all measurement points. The probability thresholds are set to 2.5% and 99%, in order to determine the minimum and maximum mixture fractions ($Z_{min}$ and $Z_{max}$) for all conditions, and thereby $R_Z$ and $R_\Delta$. These values are plotted in the regime diagram described in the previous section.

In a first step, the effect of the overall equivalence ratio on partially premixed flames is analyzed. The equivalence ratio is adjusted by changing the ratio of fuel and air flow, while keeping the Reynolds numbers constant. $R_Z$ and $R_\Delta$ calculated for all measurement points are plotted in the regime diagram, where the different colors indicate the three overall equivalence ratios (Figure 6). Note, information of Reynolds number and measurement position are not evident in this figure.

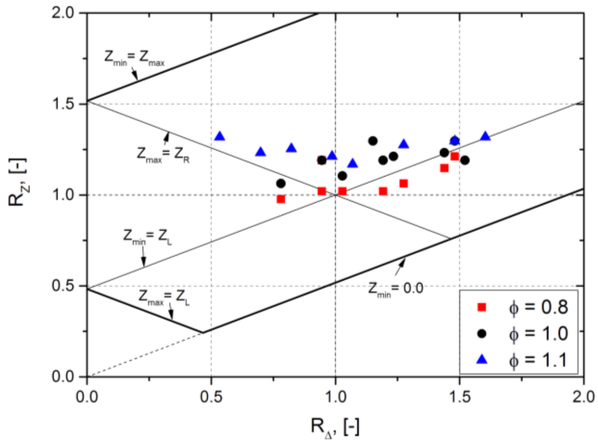


**Figure 6 Effect of equivalence ratio on partially premixed flame**

Figure 6 shows that the fluctuation of mixture fraction ($R_\Delta$) is unaffected by the equivalence ratio. While the range of $R_\Delta$ is between 0.75 and 1.5 for $\phi = 0.8$ and $\phi = 1.0$, the range is slightly increased for $\phi = 1.1$ to 0.5 – 1.6. For $\phi = 0.8$, most values are close to $R_Z = 1.0$, for higher $R_\Delta$, the $R_Z$ values are slightly higher. For $\phi = 1.0$, $R_Z$ is fluctuating around 1.15 for low $R_\Delta$ and increases for higher $R_\Delta$. $R_Z$ is independent of $R_\Delta$ for $\phi = 1.1$. Overall, the mean mixture fractions are closer to the rich flammability limit and in some cases even exceed the rich flammability limit.

In a next step, the effect of mixing on partially premixed flames is analyzed. In order to vary the time for mixing, measurements are performed at three different positions above the burner exit. In Figure 7, the experimental results are plotted in the regime diagram. The colors indicate the different positions above the burner, while information on equivalence ratio and Reynolds number is not shown.

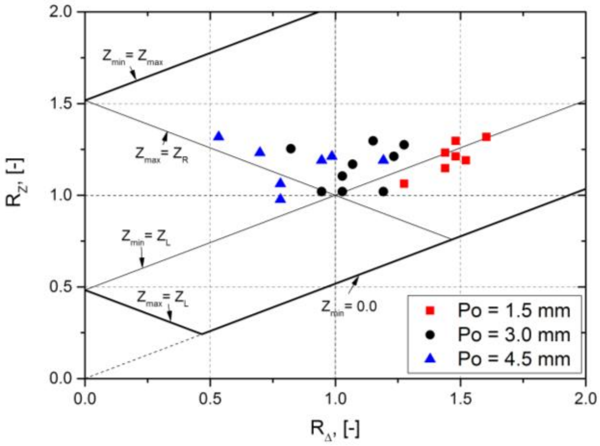


**Figure 7 Effect of time for mixing on partially premixed flame stability**

The mean mixture fraction is independent of the measurement position. As discussed above, the main influencing parameter for $R_Z$ is the overall equivalence ratio. The major effect of the measurement position, and thereby the time for mixing is related to the mixture fraction fluctuations. For the measurement position closest to the burner exit, the dimensionless fluctuations of the mixture ratio are roughly 1.5. Mixture fraction pockets are partially within the flammability limits or outside. With increasing distance from the burner exit, the fluctuations decrease. For a measurement position 4.5 mm above the burner, the fluctuations are low enough that all observed points are located in the most stable partially premixed regime inside the flammability limits (PP-IFL). Here, the increasing time for mixing increases the stability of partially premixed flames.

In a further step, the effect of the Reynolds number on the stability of partially premixed flames is discussed. The overall Reynolds number is varied by increasing the exit velocity at the main slit exit, while the equivalence ratio remains constant. In Figure 8, the color of the symbols in the regime diagram indicates the three Reynolds numbers investigated in this study. The mixture fraction fluctuation $R_\Delta$ cover a wide range, but a dependence of the Reynolds number is not evident. Also, the influence of the Reynolds number on the partially premixed flame stability is insignificant. Therefore, an effect of the Reynolds number on the partially premixed flames is not observed.

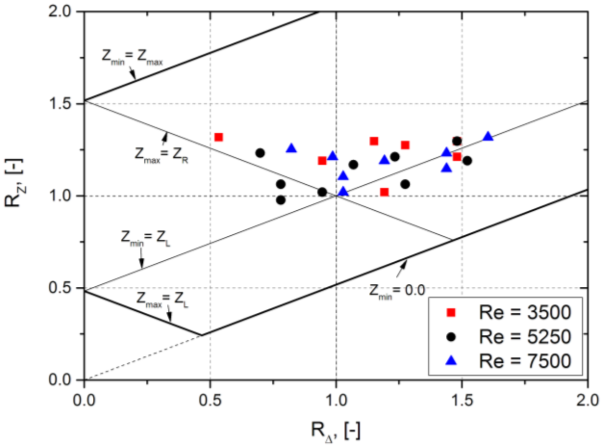


**Figure 8 Reynolds number effect on partially premixed flames**

## Conclusion

In this study, partially premixed flames were investigated in a modified, turbulent slot burner configuration to evaluate the effects of Reynolds number, equivalence ratio, and mixing time scales on the behavior and stability of this flame type. The mean mixture fraction and the mixture fraction fluctuations are appropriate quantities to characterize the flame behavior in a regime diagram, which is briefly discussed in this paper.

Simultaneous, one-dimensional Raman/Rayleigh measurements were performed in order to determine temperature and species concentrations at various positions above the burner. Three different Reynolds numbers, three different equivalence ratios and three different measurement positions were investigated. Afterwards, the experimental results were analyzed concerning the temperature-conditioned mean mixture fraction and mixture fraction fluctuation in the unburnt region and plotted in the regime diagram.

In a first step, the effect of the equivalence ratio on partially premixed flames was investigated. While the mean mixture fraction increases with increasing equivalence ratio, the mixture fraction fluctuations are unaffected.

For investigating the influence of mixing time on the partially premixed flame stability, measurements were performed at different heights above the burner. While experimental data close to the burner exit indicate high mixture fraction fluctuations ranging also outside the flammability limit, the flame stability is higher further downstream of the burner. For the highest position above the burner, the mixture fractions are located within the flammability limit.

In a last step, the effect of the Reynolds number on the stability of partially premixed flames is evaluated. The, influence of the Reynolds number on the mean mixture fraction and the mixture fraction fluctuation is insignificant. For the stability of partially premixed flames, the mixing process is the determining parameter.


## Acknowledgement

This research was performed as part of the collaborative research center SFB 686, which is funded by the German Research Association (Deutsche Forschungsgemeinschaft (DFG)). The support is gratefully acknowledged.


## References


[1] M. S. Mansour, *9th Mediterranean Combustion Symposium*, 2015.

[2] S. B. Pope, *Ann. Rev. Fluid Mech. 19*, pp. 237-270, 1987.

[3] S. Meares and A. R. Masri, *Combust. Flame 161 (2)*, pp. 484-495, 2014.

[4] I. N. Bishop and A. Simko, *SAE paper 680041*, 1968.

[5] R. A. Hasalett, M. L. Monaghan and J. J. McFadden, *SAE paper 760755*, 1976.

[6] A. R. Masri, *Proc. Combust. Inst. 35, in print*, 2015.

[7] N. Peters, Turbulent Combustion, Cambridge: Cambridge University Press, 2000.

[8] R. Borghi, *Prog. Energy Combust. Sci. 14*, 1988.

[9] N. Peters, "ERCOFTAC summer school on Laminar and Turbulent Combustion," 1992.

[10] F. Seffrin, F. Fuest, D. Geyer and A. Dreizler, *Combust. Flame 157*, p. 384–396, 2010.

[11] M. S. Sweeney, S. Hochgreb, M. J. Dunn and R. S. Barlow, *Combust. Flame 159*, p. 2912–2929, 2012.

[12] A. R. Masri, R. W. Dibble and R. S. Barlow, *Prog. Energy Combust. Sci. 22*, p. 307–362, 1996.

[13] A. R. Masri and R. W. Bilger, *Proc. Combust. Inst. 21*, p. 1511–1520, 1988.

[14] M. S. Mansour, *Combust. Sci. Tech. 152*, pp. 115-145, 2000.

[15] R. S. Barlow, G.-H. Wang, P. Anselmo-Filho, M. S. Sweeney and S. Hochgreb, *Proc. Combust. Inst. 32*, pp. 945-953, 2009.

[16] M. S. Mansour and Y.-C. Chen, *Appl. Optics 35 (21)*, pp. 4252-4260, 1996.